


HOVER PERFORMANCE ANALYSIS OF COAXIAL MINI UNMANNED AERIAL VEHICLE FOR APPLICATIONS IN MOUNTAIN TERRAIN

Ramesh P. S. , Jeyan J. V. MURUGA LAL 

Department of Aerospace, Lovely Professional University, 144411 Jalandhar, India

Received 25 June 2021; accepted 9 October 2021

Abstract. Due to its compactness, agility, good hover performance, and ease of carriage, coaxial rotor Mini UAV is apt for various military and civilian applications in mountain terrain. This paper examines various factors to arrive at viable configurations of coaxial rotor Mini UAV for applications in mountain terrain. A consideration of the coaxial rotor Mini UAV to analyse the suitability for mountain terrain is presented. Coaxial rotor design is evaluated to assess the design requirements of mountain terrain. Various design parameters are analysed to arrive at viable design configurations for coaxial rotor Mini UAVs to operate in mountain terrain. Due to mechanical complexities, more than three blades per rotor for a small coaxial rotary wing aircraft is not recommended. The compact frame of the coaxial rotor Mini UAV is a key advantage, so rotor blades with a radius bigger than 1 m are not desirable. With a radius smaller than 1 m, a range of 0.9 m to 1.2 m, and an rotor speed between 900 RPM and 1200 RPM for 3-blade and 2-blade coaxial rotors, the Mini UAV offers a variety of options for applications in mountain terrain.

Keywords: Mini UAS, Mini UAV, UAV design, UAS applications, rotary wing UAV, coaxial rotor Mini UAV.

Introduction

Unmanned aerial vehicle (UAV) is the airborne subsystem of an unmanned aircraft system (UAS) that includes necessary equipment, network, and personnel to control an unmanned aircraft (US Department of Defense, 2013). Based on the analysis of the works of various authors and data from manufacturers, the authors in Ramesh and Jeyan (2020) classified the Mini UAVs. The quantified parameters are range, 30–40 kilometers, operating altitude of approximately 3500 meters above mean sea level (AMSL), endurance, 3–4 hours, and (maximum take-off weight) MTOW of 30 kg. Mini UAVs are essentially man-portable and field-deployable UAVs used by mobile battle groups and for a variety of civil applications (Hobbs, 2010; González-Jorge et al., 2017; Jha, 2016; Valavanis & Vachtsevanos, 2015).

The current generation of Mini UAVs includes fixed wing, rotary wing, and hybrid air vehicles. The analysis by Ramesh and Jeyan (2021), concludes that Mini UAV operations in mountain terrain is the most challenging. The ability to take off and land from almost anywhere, superior hover efficiency, and maneuverability provide distinct advantages to the rotary wing Mini UAVs in mountain terrain. Rotary wing configurations include conventional

main rotor-tail rotor, coaxial rotors, tandem rotors and synchropters. The most common helicopter configuration, also called the conventional helicopter, consists of one main rotor as well as a tail rotor to the rear of the fuselage. A coaxial rotor configuration comprises an upper and a lower rotor that rotate in opposite directions. Since torque balance is achieved with contra-rotating the main rotor system, a tail rotor is not required. Coaxial rotor UAVs have sparked considerable interest in recent times due to their compactness, aerodynamic symmetry, and other design features. Although the coaxial rotor configuration is popular in the smaller micro air vehicle (MAV) category, Mini UAVs with coaxial rotors are scarce and the existing coaxial rotor UAVs do not conform to the parameters for a Mini UAV. Recent entrants include the TD220 with a maximum take-off weight (MTOW) of 290 kg, the FL-18 SkyBorg with 55 kg MTOW, the Birotor with 245 kg MTOW, and the VRT 300 with 350 kg MTOW. However, these aircraft, because of high MTOW, cannot be classified as Mini UAV. IT180-3EL-I UAV, despite having MTOW of 24 kg, suffers from low endurance of less than an hour.

Research on small coaxial rotor UAVs have been largely limited and primarily confined to numerical analysis, modelling and experiments, mostly confined to MAVs.

*Corresponding author. E-mail: psramesh1026@gmail.com

Table 1. Research on coaxial rotor UAV

Author	Research object	Research focus
(Bohorquez et al., 2003)	Micro-coaxial rotorcraft weighing approximately 100 grams.	Feasibility of achieving hover and fully functional flight control of the MAV.
(Chen & McKerrow, 2007)	Radio-controlled coaxial toy-helicopter Lama.	Develop a dynamic model to study control issues of coaxial rotors.
(Bohorquez, 2007)	112 mm rotor radius MAV.	Hover performance using computational fluid dynamics (CFD) analysis.
(Lakshminarayan & Baeder, 2009)	MAV weighing 100 grams.	Computational investigation of rotor aerodynamics in hover.
(Lee, 2010)	Ducted contra-rotating 14 inches coaxial rotor diameter MAV.	Experimental study to investigate the performance of a ducted coaxial rotor system at MAV scales.
(Prior & Bell, 2011)	Various MAVs.	Inter-rotor spacing attribute of a co-axial rotor system.
(Cui et al., 2012)	MAV with rotor diameter of 0.7 m and weighs 990 g without battery.	Construction and modelling of a variable collective pitch coaxial UAV for in-forest operation.
(Singh & Venkatesan, 2013)	MAV with diameter of 340 mm weighing 195 g.	Experimental performance evaluation of coaxial rotors for a MAV.
(Wang et al., 2015)	MAV with a rotor radius of 0.125 m.	Flight dynamics modelling of coaxial rotorcraft.
(Harun-Or-Rashid et al., 2015)	0.76 m radius coaxial rotor MAV	Nonuniform inflow model for the lower rotor of a coaxial rotor helicopter in forward flight.
(Yuan & Zhu, 2015)	3.81 m radius coaxial rotor UAV	Mathematical model for experimental analysis for dynamic analysis.
(De Giorgi et al., 2017)	Coaxial rotor UAV	Numerical simulation using CFD toolbox for performance analysis characterized by a relevant axial distance and a variable pitch.
(Mokhtari et al., 2017)	Coaxial rotor UAV	Numerical simulations and modelling to demonstrate the efficiency of the proposed hierarchical controller for coaxial-rotor UAV.
(Thiele et al., 2019)	Coaxial rotor UAV	Aerodynamic calculation of coaxial counter-rotating rotors is carried out and the knowledge gained is used to analyse a wingtip pusher propeller configuration.
(Ong et al., 2019)	Coaxial rotor UAV	Design issues related to coaxial rotor UAVs with heavy lift capabilities.

Compared to Mini UAVs, MAVs have limited capabilities because of their smaller size. Details of research on coaxial rotor unmanned vehicles over the past two decades are given in Table 1.

There are many other studies related to coaxial rotors, but the focus is on MAVs. Conversely, studies with respect to the application of Mini UAVs with a coaxial rotor configuration are negligible. As seen from Table 1, coaxial rotors as an option for small UAVs have been under active consideration for almost two decades. However, in the initial days, there was a predominant bias towards MAVs. In most contemporary studies related to coaxial rotors, the focus has shifted to numerical analysis, modelling, and CFD analysis with aerodynamic optimisation of the coaxial rotors as the central objective. However, due to practical considerations for applications, an optimum aerodynamic solution may not necessarily be the best workable solution. In the case of coaxial rotor Mini UAVs, research on aspects related to the mission or applications is negligible, and at best the application part finds only a passing mention in various studies. The purpose of this paper is to analyse various design options for a coaxial rotor Mini UAV for applications specifically for mountain terrain.

1. Consideration of coaxial rotor Mini unmanned aerial vehicle for mountain terrain

Compactness of coaxial rotors has few distinct advantages for Mini UAVs in mountain terrain, particularly for military applications. Some of the significant advantages are as under:

1. Provides the ability to manoeuvre in restricted spaces; a critical factor in combat conditions.
2. The compact frame presents itself as a smaller target against enemy fire.
3. Ease of carriage in rugged terrain where movement is by foot.

The main advantages and disadvantages of co-axial rotor systems are discussed below (Wang et al., 2015; Leishman & Ananthan, 2008; Prior & Bell, 2011).

1.1. Advantages of coaxial rotor Mini unmanned aerial vehicle for mountain terrain

1. The lack of a tail rotor is the single biggest advantage of the co-axial rotor arrangement for a multitude of reasons. The tail rotor of a singular rotor system

consumes up to an estimated 5–10% and at times 20% of the total power supplied by the engines. Due to the absence of tail rotor, no power is wasted for anti-torque or directional stability. The entire power from the coaxial rotors is used for the vertical thrust.

2. The absence of a tail rotor and tail boom results in an aircraft that is smaller and lighter. For the same weight of the helicopter, the coaxial helicopter can be 35–40% smaller than a single-rotor helicopter. The shorter fuselage reduces the visual signature, and the aircraft presents itself as a smaller target against enemy fire for military applications.
3. In order to counter the main rotor torque, the tail rotor with a much smaller radius requires high rotational speed. The high rotational speed results in high audio signature, an undesirable feature under combat conditions.
4. Due to the exclusion of the tail rotor, a major cause of helicopter accidents is eliminated. The ability to manoeuvre in restricted spaces is enhanced because there is no possibility of a tail rotor strike.
5. Piloting is much simplified due to the compactness, aerodynamic symmetry, and lack of cross connections in the control channel, which is especially important for flights at low altitude and near obstacles.
6. Folding compactness, construction simplicity, and packaging ease are aided by aerodynamic symmetry and a shorter fuselage. These are critical considerations when the air vehicle is required to be deployed in rugged terrain.
7. Since there is no large mass hanging in the rear, because of the absence of a tail boom, there is a reduction in the angular momentum. The effect this has on aircraft capability is that faster, more accurate turns can be accomplished, thereby increasing the agility and manoeuvrability.
8. The contra-rotating rotors significantly reduce retreating blade stall, resulting in an increase in high-speed directional stability. UAVs with a coaxial configuration of rotors have a considerably larger range of slip angles, rotation rates, and accelerations over the entire range of flight speeds.
9. Coaxial configuration is not impacted by crosswinds due to the absence of loss of tail rotor effectiveness. High speed wind blowing through the tail rotor in the direction it is blowing air results in loss of efficiency. In such a scenario, the rotor pitch needs to be increased, possibly leading to a tail rotor stall. This indifference in case of coaxial rotors, coupled with the absence of a tail rotor, allows for ultra-low level operations around obstacles.

1.2. Disadvantages of coaxial rotor Mini unmanned aerial vehicle for mountain terrain

1. Complex design of the linkages increases the complexity of manufacturing. Inter rotor spacing and main gear drives are other key design challenges.
2. Software design for a coaxial rotor UAV is more challenging because of the complexity of control linkages. Consequently, quicker response and accuracy of the control algorithm becomes a critical design factor for the air vehicle.
3. The upper rotor swirl impinging on the lower rotor reduces the thrust generated by the lower rotor. Therefore, the pitch angle has to be trimmed at a higher setting. This, in turn, would limit the range of the pitch angle of the upper rotor, resulting in lowering the overall efficiency of the rotor system.
4. Assembling the air vehicle will take longer and demand more skill due to the complexity of the links. The operational crew must be well trained to construct and disassemble the plane under field conditions.
5. Cost of manufacturing and maintenance, vibration issues and higher rotor drag are some other major disadvantages.

2. Analysis of design requirements of coaxial rotor Mini unmanned aerial vehicle for mountain terrain

2.1. Blade element momentum theory as the basis

Harrington's wind tunnel experimental study on two full scale coaxial rotor performances (Harrington, 1951), conducted seventy years ago, continues to be a very useful benchmark, against which the performance of interacting rotors can be evaluated. Andrew (1980), analysed the coaxial rotors with a computer wake model based on blade element, momentum and vortex theories. The results obtained from the computer model using BEMT compared favourably with earlier experimental results and the wake model. Saito and Azuma (1981), carried out an extensive numerical evaluation of coaxial rotors using blade element momentum theory (BEMT). The results obtained were in consonance with previous experimental results.

Leishman and Ananthan (2008) developed and derived the momentum theory and the BEMT analysis for coaxial rotor systems, extensively using Harrington results to validate BEMT outcomes. The analysis exhibited very good consistency with experimental results. Rand and Khromov (2010), presented aerodynamic optimization of a coaxial rotor system in hover and axial flight based on BEMT using real nonlinear aerodynamic tables. Yana and Rand (2012), investigated the coaxial rotor system in hover, using BEMT as the common basis for three varied points of view. As per Leishman and Syal (2008), BEMT serves as a good benchmark for analysis of coaxial rotor system performance over a given operational thrust range. Ramasamy (2013) used BEMT to compare and contrast the measurements of a torque-balanced coaxial rotor against predicted values with a single-rotor system with equivalent solidity.

Therefore, it is seen BEMT has been extensively used in predicting the outcome of a coaxial rotor system.

BEMT is mathematically parsimonious, computationally expedient, and reasonably well-validated against performance measurements. Furthermore, the BEMT results give a solid modelling foundation for developing a rotor design solution that can be investigated further utilising computational and experimental methodologies. Hence, for the design evaluation of critical parameters, BEMT is used as the basis.

2.2. Maximum take-off weight

Due to the advancement in communication technology, most Mini UAS can easily operate at a range of 30–40 km. But with the current technology, an endurance of 3–4 hours is unlikely to be achieved by battery-operated UAVs. Therefore, the Mini UAV has to be engine powered to meet the endurance requirement. Engine power degrades as altitude increases and dips significantly in the region of 3500 m AMSL. On the other hand, the thrust generated by the rotors will also drop considerably, due to the rarefied atmosphere. Consequently, the Mini UAV design has to cater for adequate reserve power. MTOW of 30 kg is not a critical design factor for Mini UAS operations in terrain that facilitates vehicular movement. However, for rugged terrain like mountains, wherein the movement has to be on foot, the weight of the UAV becomes a criticality. The weight of the other components of the system like the GCS, datalink, payload and technical support systems also needs to be factored (Ramesh & Jeyan, 2021). Since the entire UAS has to be physically carried by the operating crew, MTOW in excess of 20 kg for the Mini UAV is not desirable.

2.3. Thrust

As seen from the thrust equation for hover (Prouty, 2002), given in Eq. (1), there are a number of variables associated with rotary wing aerodynamics. For vertical climb, the climb velocity also needs to be considered and resultant additional power requirements:

$$T = \frac{\rho}{2} (\Omega R)^2 N_b c R a \left(\frac{\theta_t - \phi_t}{2} \right) = \frac{C_T}{\sigma} \rho N_b c R (\Omega R)^2, \quad (1)$$

where $\sigma = \frac{N_b C}{\pi R}$.

As seen from Eq. (1), to produce the desired thrust, the blade pitch is affected by the induced velocity, density, rotor speed and rotor radius. The thrust generated by the helicopter has to compensate for a number of losses. Loss due to induced flow, profile drag and parasite drag has to be taken into consideration. Additional losses due to non-uniform flow, swirl in the wake, tip losses, and blade root cut out also need to be factored (Venkatesan, 2015). Although there are no losses due to the tail rotor in a coaxial configuration, losses due to rotor-on-rotor interference are significant. The interference losses can be in excess of 20%, which can be reduced to some extent by increasing the gap between the rotors (Leishman & Syal, 2008). Taking into account all of the aforementioned factors, the Mini UAV

design should allow for a thrust of at least 30 kg at 3500 m AMSL. Therefore, in the current analysis, calculations will be based on 30 kg thrust.

2.4. Blade radius

More often than not, the UAV will have to be dismantled and carried to the deployment site and then assembled for operations. For ease of carriage and packaging, rotor blade length beyond 1 m is not desirable. A longer blade also increases the vulnerability to enemy fire in a combat environment. Hence, a 1 m blade radius has been considered as the benchmark for the analysis.

2.5. Number of blades

Increasing the number of blades will facilitate a design with a lower rotor n and/or smaller rotor radius. Each blade will be lighter and easier to handle as the number of blades increases. More blades per rotor in the case of a coaxial configuration will result in more mechanical linkages, an undesirable outcome. A design with higher n can be made more compact with a smaller rotor radius and/or with fewer number of blades. Vibration sensitivity, acoustic signature, and wear and tear are all negatively impacted by increased n . Increasing the radius can result in lower n and lesser number of blades, but this will be at the cost of the compactness of the air vehicle. Considering all these factors, it is obvious that there cannot be one coaxial rotor design that can operate at a lower n , smaller radius, and with a fewer number of blades. Therefore, the optimum design has to strike a balance between the number of blades, radius, and rotor speed to produce the required thrust at a certain altitude ceiling. Due to the mechanical complexities involved with more than three blades per rotor for a small coaxial rotary wing aircraft, further analysis will be based on comparison between two and three blades per rotor.

2.6. Ratio of rotor separation distance to the rotor diameter

One critical aspect for consideration specific to a coaxial rotor system is the ratio of rotor separation distance to the rotor diameter, H/D . Analysis by Lim et al. (2009), exhibited that the coaxial rotor spacing effect on hover performance was insignificant for rotor spacing larger than 20% of the rotor diameter. In the investigations by Prior (2010), it was found that although large manned aircraft use an H/D ratio of around 0.1, small UAVs employing co-axial rotors tend to have much higher ratios of between (0.25–0.47), implying a scaling effect. In a later study, Prior and Bell (2011) analysed the H/D ratio of a small UAV, studying the performance of these systems at incremental stages. They concluded that H/D ratios in the region of (0.41–0.65) are advantageous in the performance of small UAVs. In the experimental study on micro air vehicles by Lei et al. (2018), results showed that the optimal performance for a coaxial rotor system is obtained with a

H/D of 0.19. One common factor emerging from various studies is that the rotor-on-rotor interference does contribute to thrust loss in a coaxial rotor system, but the interference is reduced with increased spacing. Hence, H/D greater than 0.25 is considered for the current study.

2.7. Correlation between coaxial rotors and equivalent single rotor

The relationship between pitch and thrust is given by (Prouty, 2002),

$$\theta_t = 57.3 \left[\frac{4}{a} \frac{C_T}{\sigma} + \sqrt{\frac{C_T}{2}} \right] \text{degrees.} \quad (2)$$

Since the coaxial rotor essentially behaves as two isolated single rotors or an equivalent single rotor, evaluations can be done in terms of an equivalent single rotor. In order to compare a single and coaxial rotor, the rotors have to be identical in terms of geometry and also the operating conditions. By keeping the same number of blades N_b , disc loading $\frac{T}{A}$, rotor solidity σ , and tip speed V_{tip} , Fernandes (Fernandes, 2017), developed a set of equations. These equations were validated with the experimental results of Harrington Rotor 2.

For a coaxial rotor and equivalent single rotor with equal disk loading (DL),

$$(DL)_{coax} = (DL)_{eq}, \frac{T}{A_{coax}} = \frac{T}{A_{eq}}, A_{eq} = 2A^u.$$

$$\text{Since } A^u = A^l, \text{ therefore, } R_{eq} = \sqrt{2} R^u = \sqrt{2} R^l. \quad (3)$$

For equal rotor solidity between coaxial and equivalent single rotors, the rotor blades will have different chord lengths, $\sigma_{eq} = 2\sigma^u = 2\sigma^l$. Since, $\sigma_{coax} = 2\sigma^u = 2\sigma^l$, therefore, $c_{eq} = \sqrt{2} c^u = \sqrt{2} c^l$.

As evident from Eq. (3), the radius of the equivalent single rotor will be greater than that of the coaxial rotor. For equal n for both the rotor systems, the tip speed will be different. In order to obtain the same tip speed for the two rotors, the n between the two systems has to be adjusted,

$$(V_{tip})_{eq} = (V_{tip})_{coax}, \Omega_{eq} R_{eq} = \Omega_{coax} R_{coax} \text{ or } \Omega_{eq} = \frac{\Omega_{coaxial}}{\sqrt{2}}. \quad (5)$$

The above equations are for hover conditions and do not consider non-uniform flow, tip losses, blade twist, and inter rotor interference. A rotor that is optimised for best hover performance must have minimum induced and profile power losses to produce the best performance. For minimum induced power, the flow has to be uniform. To ensure minimum profile power, each blade section operates at its optimum condition with a maximum value of $\frac{C_l}{C_d}$. These two criteria define the twist and taper for

the optimum rotor to obtain the best hover performance. However, due to manufacturing considerations, most rotor blades have a constant chord over a major portion of the rotor blade.

2.8. Significance of torque balanced state and thrust sharing ratio

Leishman and Syal (2008), examined four primary cases of interest for a coaxial rotor system. For each case, rotor-on-rotor interference losses for coaxial rotors, was quantified with interference induced power factor, k_{int} . k_{int} relates the performance of a coaxial rotor system to two isolated rotors operating separately but at the same disk loading as for the two rotors of the coaxial system. The case where rotors are operated at balanced torque with the lower rotor operating in the vena contracta of the upper rotor, as shown in Figure 1, was found to be of primary practical importance. This is because, practical considerations in a coaxial system dictate that the rotors are sufficiently separated to prevent inter-rotor blade collisions from blade flapping. Therefore, the lower rotor generally always operates in the vena contracta of the upper rotor. For any thrust condition, the coaxial rotors must be free of any residual yawing moment. This implies that, upper and lower rotors also operate at different thrusts and different induced velocities. Hence, further analysis will be based on two rotors operating in a torque balanced state that are operated independently, but at the same thrust-sharing ratio.

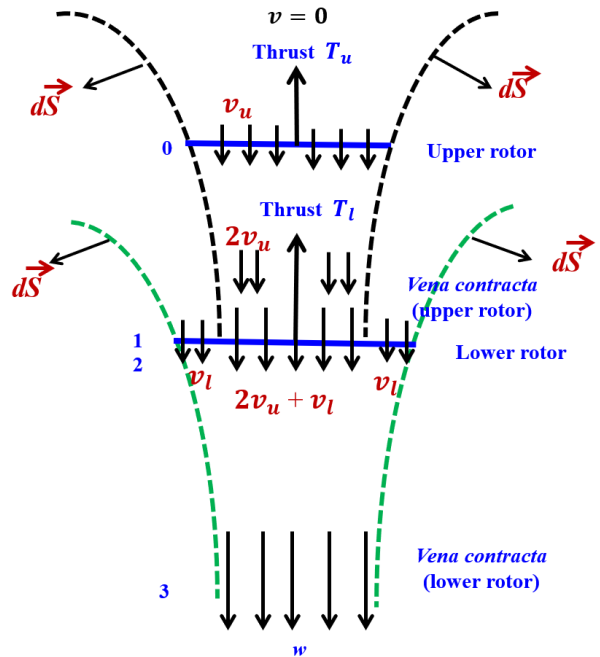


Figure 1. Flow model of coaxial rotor system with lower rotor operating in the vena contracta of the upper rotor (Leishman & Syal, 2008)

3. Analysis of design parameters of coaxial rotor Mini UAV for mountain terrain

3.1. Pitch and rotor rotation per minute

As previously alluded to, a compact frame is amongst the key design parameters for Mini UAVs operating in mountain terrain. The lesser the blade radius, the more compact will be the coaxial rotors. As a benchmark, the radius for the hover condition has been kept constant at 1 m. The $\Theta - n$ correlation for 2-blade and 3-blade coaxial rotor systems at varying standard densities from mean sea level to 3500 m AMSL is as shown in Figure 2a and Figure 2b, respectively. The graphs have been arrived at, based on an equivalent single rotor for a coaxial rotor to support the thrust of 30 kg. On an average, the maximum collective pitch for main rotors for helicopters is in the region of 12–15°. But the collective pitch is often operated well below the maximum limit in order to cater for reserve power.

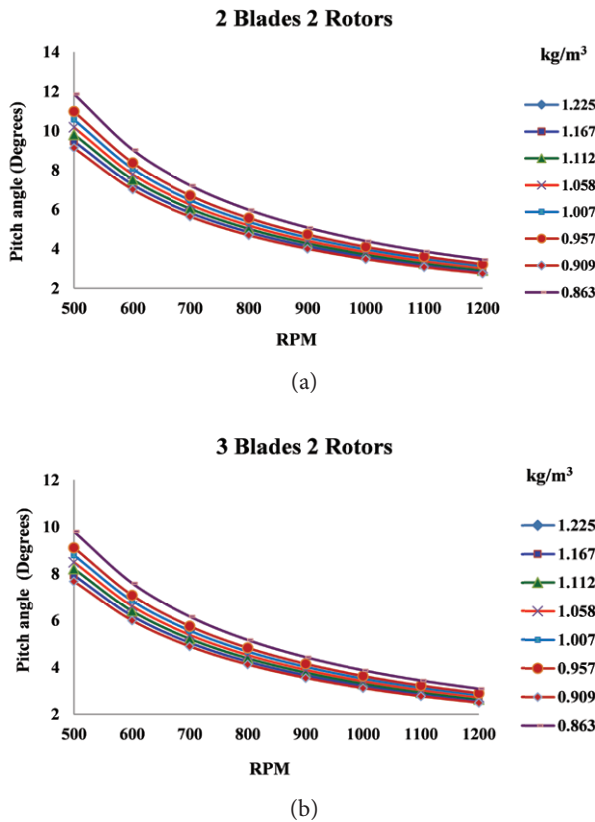


Figure 2. $\Theta - n$ relation for 2-blade 2 rotor and 3-blade 2 rotor coaxial rotor systems

3.2. Pitch and rotor radius

The pitch-radius relationship at various n for 2-blade and 3-blade coaxial rotor systems are as shown in Figure 3a and Figure 3b, respectively. Since the air vehicle is expected to operate at 3500 m AMSL, standard density at that altitude has been considered. The graphs are based on an equivalent single rotor for a coaxial rotor subjected to a thrust of 30 kg. Although a higher radius provides

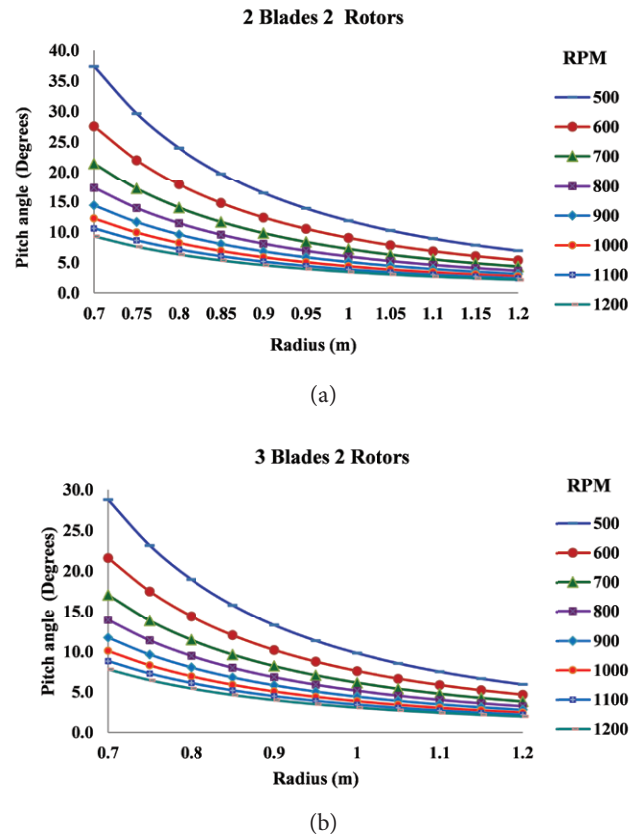


Figure 3. Pitch – Radius relation for 2-blade 2 rotor and 3-blade 2-rotor coaxial rotor systems

better performance, radius in excess of 1 m is not desirable due to compactness considerations. In order to maintain a lower radius, the rotor speed has to be higher.

3.3. Thrust sharing ratio

The mass flow rate of air passing through the upper rotor is ρAv_u . Therefore, the momentum flux exiting in the slipstream of the upper rotor is

$$(\rho Av_u)2v_u = 2\rho Av_u^2 \tag{6}$$

Eq. (6) represents the momentum flux of the air entering the lower rotor. The mass flow rates over the inner and outer parts of the lower rotor are $\rho\left(\frac{A}{2}\right)(2v_u + v_l)$ and $\rho\left(\frac{A}{2}\right)v_l$, respectively. Hence, the net mass flow rate through the lower rotor is, $\dot{m} = \rho\left(\frac{A}{2}\right)(2v_u + v_l) + \rho\left(\frac{A}{2}\right)v_l = \rho A(v_u + v_l)$. Assuming uniform velocity, the momentum flux through plane 3

(Figure 1) is $\dot{m}w_l$. Therefore, the thrust on the lower rotor is, $T_l = \rho A(v_u + v_l)w_l - 2\rho Av_u^2$. Power or the work per unit time done on the air by the lower rotor is

$$P_l = T_l(v_u + v_l) \tag{7}$$

This is equal to the gain in kinetic energy of the air in the slipstream. Therefore,

$$P_l = T_l (v_u + v_l) = \frac{1}{2} \rho A (v_u + v_l) w_l^2 - \frac{1}{2} \rho A 2v_u (2v_u)^2.$$

Hence, $P_l = \frac{1}{2} \rho A (v_u + v_l) w_l^2 - 2\rho A v_u^3.$ (8)

For torque balanced case with equal rotor rotational and tip speeds, $P_u = P_l$.

Hence, $T_u v_u = T_l (v_u + v_l);$ (9)

Multiplying Eq. (9) by $v_u (v_u + v_l)$ and rearranging,

$$P_l (2v_u + v_l) = \rho A (v_u + v_l)^2 v_u w_l.$$
 (10)

For torque balanced state, $P_u = 2\rho A v_u^3 = P_l$. From Eq. (7) and Eq. (8),

$$P_l = \frac{1}{4} \rho A (v_u + v_l) (w_l)^2.$$
 (11)

Substituting the value of P_l from Eq. (11) in Eq. (10) and rearranging,

$$w_l = 4v_u \left(\frac{v_u + v_l}{2v_u + v_l} \right).$$
 (12)

Using $P_u = 2\rho A v_u^3 = P_l$, and substituting the values from Eq. (12) and Eq. (9) into Eq. (10),

$$P_l = 2\rho A v_u^3 = 8\rho A (v_u + v_l) v_u^2 \frac{(v_u + v_l)^2}{(2v_u + v_l)^2} - 2\rho A v_u^3.$$
 (13)

Solving the equation, $v_l = 0.4375 v_u$. For a torque balanced condition, $T_u v_u = T_l (v_u + v_l)$.

Therefore, the thrust sharing ratio between the upper and lower rotor for a torque balance condition is,

$$\frac{T_u}{T_l} = 1.4375.$$
 (14)

This implies that all other parameters being the same, the upper rotor will have a higher mean lift coefficient and higher pitch. Therefore, the collective pitch angles arrived at in Figure 2 and Figure 3 do not provide the correct perspective. Since the upper and lower rotors operate at different thrusts, it would be prudent to compare the the 2-blade and 3-blade coaxial rotor systems on the basis of the mean lift coefficient C_l , separately for upper and lower rotors.

3.4. Mean lift coefficient and rotor rotation per minute

The equation for the mean lift coefficient (Venkatesan, 2015), is given by

$$\overline{C_l} = \frac{6C_T}{\sigma}.$$
 (15)

The relationship between mean lift coefficient $\overline{C_l}$ and n for varying radius for 2-blade coaxial rotors is as shown in Figure 4a and 4b and that for 3-blade coaxial rotors is as shown in Figure 5a and 5b. All calculations are based on

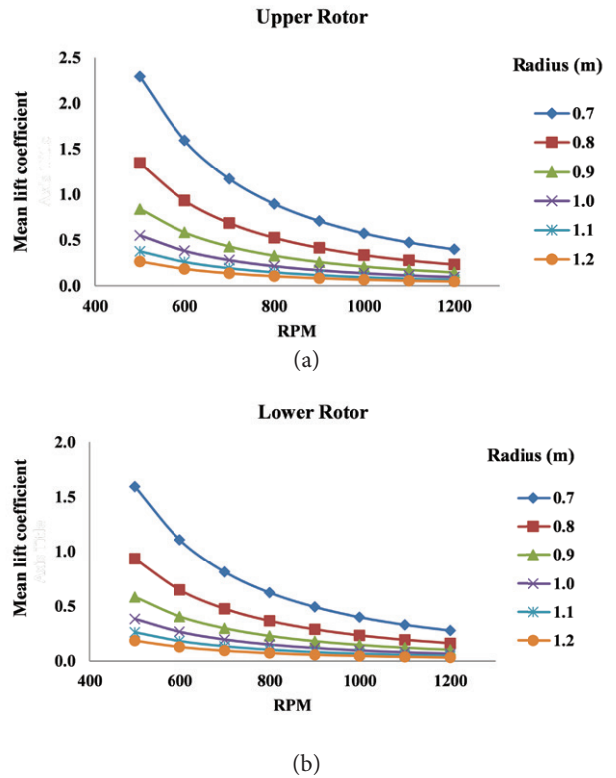


Figure 4. $\overline{C_l} - n$ relation for 2-blade 2 rotor at various radiuses for upper and lower rotors

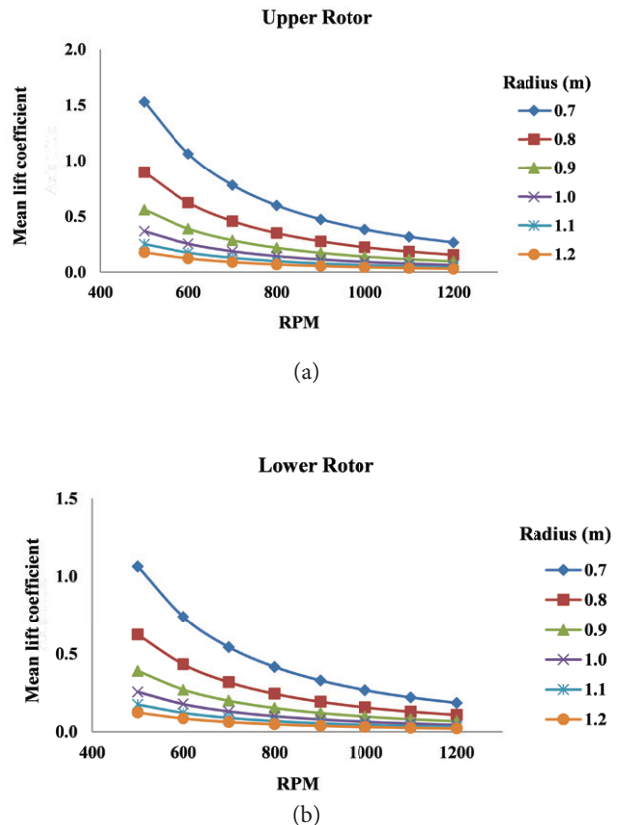


Figure 5. $\overline{C_l} - n$ relation for 3-blade 2 rotor at various radiuses for upper and lower rotors

standard density at 3500 m AMSL and the thrust requirement of 30 kg. As seen from the figures, the coefficient of lift for the upper rotors in both the configurations is significantly higher than the lower rotor. This implies that the upper blades will stall earlier than the lower blades.

Usually, for helicopters, the rotors operate at C_l between 0.35 and 0.6 (Prouty, 2002; Venkatesan, 2015). As seen from Figure 4 and 5, the blades of the upper rotor for the 2-blade 2 rotor configuration have to operate at a higher C_l than the 3-blade configuration to produce the same thrust.

3.5. Coefficient of thrust and coefficient of power

On the basis of BEMT, the equation for coefficient of power for a coaxial rotor system is as given in Eq. (16) (Leishman & Syal, 2008),

$$C_P = \frac{k_{int} k (C_{Tu} + C_{Tl})^{3/2}}{2} + \left(\frac{\sigma C_{d0}}{4} \right). \quad (16)$$

Figure 6a and 6b show the performance polars for 2-blade and 3-blade coaxial rotor systems at various n . These values are for 3500 m AMSL and for a thrust to support 30 kg. The coefficients have been calculated by keeping the n constant and incrementally increasing the rotor radius from 0.7 m to 1.2 m.

For the two rotors operating independently in a torque balanced state and with the same thrust-sharing ratio k_{int} , is 1.28. The induced power factor for a single

rotor k , is 1.1, based on Harrington Rotor 2 (Leishman & Syal, 2008). The zero-lift drag coefficient, C_{d0} based on NACA 0012 airfoil section, is 0.011. As seen from the figures, in both cases, there is a sharp rise in C_P and C_T at lower n and lower radius. Conversely, at higher n and higher radius, the values of C_P and C_T tend to bunch up. From the analysis of the mean lift coefficient, it has been observed that low n and low radius is not desirable. From the figure of merit perspective, to be discussed in detail later in the paper, high n and high radius lead to less efficient systems. Hence, there is a requirement to balance the contradictory requirements.

3.6. Coefficient of power by solidity and coefficient of thrust by solidity

Since the two systems operate at different solidities, the blade loading coefficient, C_T/σ , provides a better understanding of the performance and a valid comparison of the hover efficiency of the two rotors. Having taken into account the constants, k , k_{int} and C_{d0} are, the net overall thrust requirement can be reduced from hitherto considered. A 15% reduction would be a reasonable estimate while accounting for other losses. Hereafter, the calculations will be based on the reduced thrust requirement. Hover performance of rotor configurations by normalising C_T and C_P by the rotor solidity at 0.9 m, 1 m and 1.1 m radius for 2-blade and 3-blade coaxial systems are as shown in Figure 7. Rotor speed is incrementally

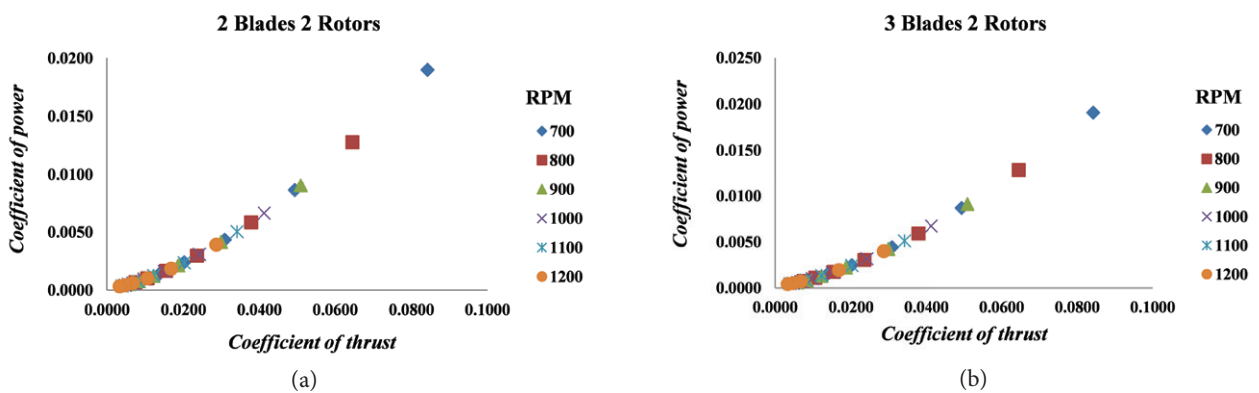


Figure 6. Relationship between coefficient of thrust C_T and coefficient of power C_P , for 2-blade and 3-blade coaxial rotor systems

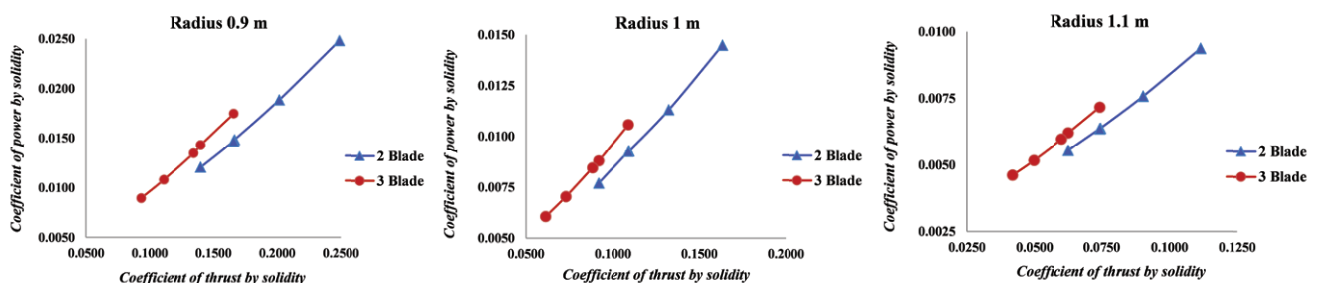


Figure 7. C_P/σ versus C_T/σ comparison for 2-blade and 3-blade coaxial rotor system

increased from 900 RPM to 1200 RPM, at fixed intervals of 100. The results are plotted in terms of, C_T/σ and C_p/σ , which gives a better perspective than system thrust and power coefficients.

It is evident from Figure 7, that the 2-blade system produces a higher total system thrust for a given power or torque. It is seen that the coefficients see a rise with a drop in n and or radius. As per Eq. (25), the blade loading coefficient, C_T/σ has implications for the mean lift coefficient, C_l . Therefore, the 2-blade coaxial system will reach the stall value of lift coefficient earlier than the 3-blade system. Typically, for contemporary helicopter rotors, the maximum realisable value of blade loading coefficient without stall is about 0.12–0.14 (Arjomandi, 2001).

3.7. Figure of merit and coefficient of thrust by solidity

Figure of merit (FM) provides a benchmark to compare the relative hovering efficiency of different rotors relative to the datum “ideal” performance provided by the momentum theory (Arjomandi, 2001; Venkatesan, 2015). While the FM is a non-dimensional parameter, it provides a basis to conduct only a relative comparison of rotor performance. FM is defined as the ratio of the ideal power required to hover to the actual power required to hover. Since the coaxial rotor system typically operates at an unequal thrust and hence at unequal disc loading at the torque-balanced condition, defining the figure of merit is

complex. Leishman and Sayal (2008), defined the figure of merit for a coaxial rotor system as per Eq. (27).

$$FM = \frac{\frac{C_T^{3/2}}{\sqrt{2}} \left[\left(\frac{C_{Tu}}{C_{Tl}} \right)^2 + 1 \right]}{k_{int} k \frac{C_T^{3/2}}{\sqrt{2}} \left[\left(\frac{C_{Tu}}{C_{Tl}} \right)^2 + 1 \right] + \frac{2\sigma C_{d0}}{8}} \quad (17)$$

Comparison of the relative performance of 2-blade and 3-blade coaxial systems is depicted in Figure 8. Full scale helicopters generally operate at a maximum FM in the range of 0.75 to 0.8. Expectedly, both the coaxial rotor configurations are less efficient when compared to single rotor systems. The values for the two rotor systems at 0.9 m, 1 m and 1.1 m have been obtained by incrementally increasing rotor from 900 RPM to 1200 RPM, at fixed intervals of 100 RPM.

3.8. Ratio coefficient of thrust to coefficient of power

Figure 9a and 9b show the ratio of coefficient of thrust C_T , to coefficient of power C_p , at various radiuses from 0.9 m to 1.2 m. The n range is from 700 RPM to 1500 RPM with an incremental increase at fixed intervals of 100 RPM. As seen from Figure 9a, for the 2-blade coaxial system,

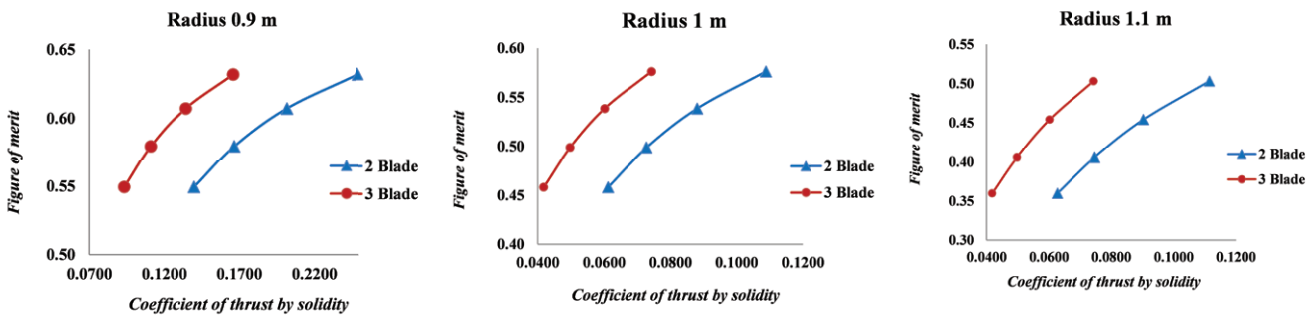


Figure 8. Blade loading coefficient, C_T/σ and Figure of Merit, FM comparison for 2-blade coaxial system and 3-blade coaxial system at various radius for 900 RPM to 1200 RPM

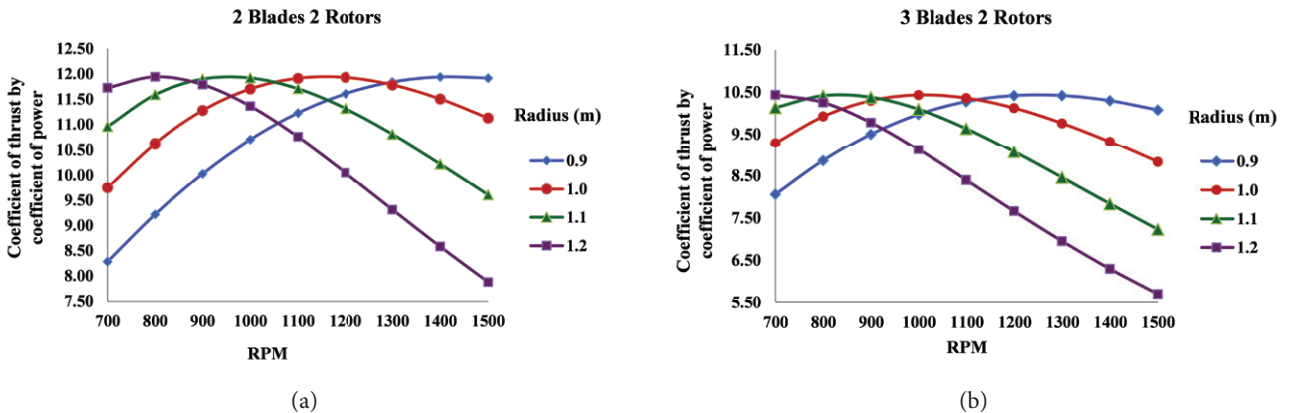


Figure 9. Ratio of coefficient of thrust C_T , to coefficient of power C_p , at various n for varying radius for 2-blade 2 rotor and 3-blade 2 rotor configurations

the peak value of C_T / C_P for 0.9 m blade radius is achieved beyond 1200 RPM at 1400 RPM. In the case of 1 m blade radius, the peak is at 1200 RPM and for 1.1 m blade radius, it is at 1000 RPM.

Peak value of C_T / C_P for 1.2 m blade radius is below 900 RPM at 800 RPM. In the case of the 3-blade system, peak value of C_T / C_P for 0.9 m blade radius is achieved beyond 1200 RPM at 1300 RPM. Peak value of C_T / C_P for 1 m is at 1000 RPM. Both 1.1 m and 1.2 blade radius operate at n below 900 RPM for peak values of C_T / C_P . In case of 1.1 m blade radius, the peak is at 800 RPM and for 1.2 m blade radius, it is at 700 RPM.

4. Findings and discussion

Coaxial rotor Mini UAVs have numerous advantages in terms of efficiency and operational capability for mountain terrain. The compact coaxial rotor frame is a significant asset for Mini UAVs, particularly for military applications. Since mountainous terrain imposes maximum restrictions on the deployment and employment of Mini UAVs, a coaxial rotor Mini UAV designed for mountains can operate in other terrains with ease.

Optimum coaxial rotor design must strike a balance between rotational speed, rotor radius and number of blades. Although it is desirable that the design should incorporate low n , small radius and lesser number of blades, contradictory requirements compel compromise between the three. Because of excessive linkages and associated mechanical complexities, more than three blades per rotor for a small coaxial rotary wing aircraft are not recommended. For rugged mountain terrain, wherein the movement has to be on foot, every gram added to the weight of the UAV becomes a criticality. Ergonomic considerations dictate that in mountains, UAVs will have to be dismantled and physically carried to the deployment site and then assembled for operations. Hence, rotor blades with a radius greater than 1 m are not recommended. Important deductions from the analysis of design requirements are (a) MTOW in excess of 20 kg for the Mini UAV is not desirable, (b) Blade length beyond 1 m is not desirable, (c) The maximum number of blades per rotor is limited to three, and (d) Two rotors operating in a torque balanced state that are operated independently, but at the same thrust-sharing ratio, is practically the most viable option.

The 3-blade arrangement is a superior alternative from the standpoint of operating altitude. At 3500 m AMSL, the collective pitch requirement at 500 RPM for a 2-blade configuration is 17% more than the 3-blade configuration. With increasing n , the gap gradually narrows until it reaches 10% at 1200 RPM. In both configurations, n below 700 RPM is undesirable. Even at 1200 RPM and 1.2 m radius, the 88.8 m/s tip speed is well within established limits. At 1200 RPM with 0.7 m radius, the collective pitch requirement for a 2-blade configuration is 12.76% more than the 3-blade configuration. As the radius is increased, the gap gradually reduces and at 1.2 m radius, the difference drops to 8.86%. For a 2-blade coaxial configuration,

radius below 0.8 m and for a 3-blade configuration radius less than 0.7 m, is not recommended.

It is evident that the upper rotor will stall much before the lower rotor in both configurations. At lower radius and RPM, the values for C_l surpass the permissible limits. As seen in Figure 4 and 5, the gain is not proportional to the increase in radius and/or n . At higher values, the improvement in performance is relatively marginal compared to the lower limits. The combination of radius greater than 0.7 m and n higher than 700 provides adequate flexibility for both blade configurations. Overall, from C_l perspective, the 3-blade coaxial exhibits better performance.

For a given power or torque, a 2 system delivers more total system thrust. If the n is reduced, the blade radius must be increased to achieve satisfactory loading coefficients. Conversely, decreasing the radius necessitates an increase in n . The rotor performance drops significantly at lower values in both configurations. In general, a radius of 0.9 to 1.1 m and rotational speeds between 900 and 1200 RPM provides adequate options.

For a given thrust, the 3-blade system is more efficient. The 2-blade system requires 33% more thrust to achieve the same FM. Since blade loading is a function of tip speed, the lower the tip speed, the higher the potential FM. Increasing the rotor n and radius decreases the FM. Therefore, it is evident that to ensure high FM, a combination of high n and low radius or vice versa has to be considered. Although the 3-blade rotor system is a better option for higher FM, both the rotor systems are acceptable with radius between 0.9 and 1.1 m and n ranging from 900 RPM to 1200 RPM.

For identical values of C_T , the value of FM will be higher with lower σ , other parameters remaining constant. For very low values of σ , the blades will have to operate at higher C_l to achieve the desired thrust. Larger C_l , can lead to early blade stall and associated increase in blade drag. This in turn can reduce the FM. From the analysis it is seen that, for a given thrust, the 3-blade coaxial rotor system has better FM. Using 3 blades per rotor leads to higher σ and hence the blade weight increases. However, considering the dimensions of the blades and MTOW for Mini UAV, the difference in blade weight between 2-blade and 3-blade configurations will be insignificant.

From Figure 9a and 9b, it is evident that the 3-blade coaxial system operates at lower thrust to power ratio when compared to the 2-blade system. In both configurations, it is only at radius below 0.9 m, the n has to exceed 1200 RPM to achieve optimum C_T / C_P ratio. Similarly, in both configurations, the n must drop below 900 to achieve the best C_T / C_P ratio. However, it is pertinent to mention that the gain in C_T / C_P ratio, beyond the envelope of 900 RPM to 1200 RPM is marginal.

Generally accepted helicopter theory envisages a decrease in tip losses with the increase in the number of blades, all other parameters remaining constant. Therefore, the 3-blade coaxial system is a better option to reduce tip losses. The 3-blade coaxial configuration also exhibits better performance in terms of C_l and FM. However, it is

seen that the 2-blade coaxial system delivers higher total system thrust for a given power or torque than the 3-blade system. For a given radius and n , the 2-blade system also has a higher thrust to power ratio.

Thus, it is seen that both the 3-blade and 2-blade coaxial systems have relative merits and demerits, providing paradoxical options. To sum up, in both configurations, the radius range of 0.9 m to 1.2 m and RPM between 900 RPM and 1200 RPM, provide multiple options. However, while considering the options, compactness or a lower rotor radius should take precedence.

Conclusions and recommendations

The design outline limiting the boundaries of radius, n , and the number of blades using BEMT presented in this paper, provide a strong modelling basis for further investigation and refinement of coaxial rotor systems design using mathematical, computational, and experimental methodologies. The current study uses a simple constant chord symmetric blade profile with no twist, taper, or tip geometry alteration. Optimising the coaxial rotor Mini UAV through analysis of different blade profiles is recommended for future work. Using different panforms for the two rotors, to minimise the thrust differential between the upper and lower rotors to improve the overall efficiency of the coaxial systems is another area that needs further investigation. Further research is planned to evaluate the 2-blade and 3-blade coaxial rotor systems to optimise radius- n combinations for both hover and axial flight conditions through mathematical modelling, CFD analysis, experimental methods, iterative processes, or a combination of the aforementioned.

Funding

The paper has not been funded.

Disclosure statement

The authors declare no conflict of interest.

References

- Andrew, M. J. (1980, September 16–19). Co-axial rotor aerodynamics in Hover, Paper No. 27. In *Sixth European Rotorcraft and Powered Lift Aircraft Forum*. Bristol, England.
- Arjomandi, M. (2001). Classification of unmanned aerial vehicles. In *Mechanical engineering*. The University of Adelaide, Australia.
- Bohorquez, F. (2007). *Rotor Hover performance and system design of an efficient coaxial rotary wing micro air vehicle* [dissertation, University of Maryland]. University of Maryland Libraries.
- Bohorquez, F., Samuel, P., Sirohi, J., Pines, D., Rudd, L., & Perel, R. (2003). Design, analysis and hover performance of a rotary wing micro air vehicle. *Journal of the American Helicopter Society*, 48(2), 80–90. <https://doi.org/10.4050/JAHS.48.80>
- Chen, L., & McKerrow, P. (2007). Modelling the lama coaxial helicopter. In *Proceedings of the 2007 Australasian Conference on Robotics and Automation* (pp. 1–9), ACRA 2007. Brisbane.
- Cui, J., Wang, F., Qian, Z., Chen, B. M., & Lee, T. H. (2012). Construction and modeling of a variable collective pitch coaxial UAV. In *Proceedings of the 9th International Conference on Informatics in Control, Automation and Robotics*, 2, 286–291. ICINCO. Rome, Italy. <https://doi.org/10.5220/0004039502860291>
- De Giorgi, M. G., Donato, T., Ficarella, A., Fontanarosa, D., Morabito, A. E., & Scalinci, L. (2017). Numerical investigation of the performance of contra-rotating propellers for a remotely piloted aerial vehicle. *Energy Procedia*, 126, 1011–1018. <https://doi.org/10.1016/j.egypro.2017.08.273>
- Fernandes, S. D. (2017). *Performance analysis of a coaxial helicopter in Hover and and forward flight*. <https://commons.erau.edu/edt>
- González-Jorge, H., Martínez-Sánchez, J., Bueno, M., & Arias, P. (2017). Unmanned aerial systems for civil applications: A review. *Drones*, 1(1), 2. <https://doi.org/10.3390/drones1010002>
- Harrington, R. D. (1951). Full-scale-tunnel investigation of the static-thrust performance of a coaxial helicopter rotor (Technical note). In *NACA TN 2318*. Defence Technical Information Center.
- Harun-Or-Rashid, M., Song, J. B., Byun, Y. S., & Kang, B. S. (2015). Inflow prediction and first principles modeling of a coaxial rotor unmanned aerial vehicle in forward flight. *International Journal of Aeronautical and Space Sciences*, 16(4), 614–623. <https://doi.org/10.5139/IJASS.2015.16.4.614>
- Hobbs, A. (2010). *Unarmed aircraft systems: UAV design, development and deployment*. Wiley. <https://doi.org/10.1016/B978-0-12-374518-7.00016-X>
- Jha, A. R. (2016). Theory, design, and applications of unmanned aerial vehicles. In *Theory, design, and applications of unmanned aerial vehicles*. CRC Press. <https://doi.org/10.1201/9781315371191>
- Lakshminarayan, V. K., & Baeder, J. D. (2009, January). Computational investigation of small scale coaxial rotor aerodynamics in Hover. In *47th AIAA Aerospace Sciences Meeting Including the New Horizons Forum and Aerospace Exposition* (pp. 1–23). Orlando, Florida. <https://doi.org/10.2514/6.2009-1069>
- Lee, T. E. (2010). *Design and performance of a ducted coaxial rotor in Hover and forward flight*. University of Maryland.
- Lei, Y., Ji, Y., & Wang, C. (2018). Optimization of aerodynamic performance for co-axial rotors with different rotor spacings. *International Journal of Micro Air Vehicles*, 10(4), 362–369. <https://doi.org/10.1177/1756829318804763>
- Leishman, J. G., & Ananthan, S. (2008). An optimum coaxial rotor system for axial flight. *Journal of the American Helicopter Society*, 53(4), 366–381. <https://doi.org/10.4050/JAHS.53.366>
- Leishman, J. G., & Syal, M. (2008). Figure of merit definition for coaxial rotors. *Journal of the American Helicopter Society*, 53(3), 290–300. <https://doi.org/10.4050/JAHS.53.290>
- Lim, J. W., McAlister, K. W., & Johnson, W. (2009). Hover performance correlation for Full-Scale and model-scale coaxial rotors. *Journal of the American Helicopter Society*, 54(3). <https://doi.org/10.4050/JAHS.54.032005>
- Mokhtari, M. R., Cherki, B., & Braham, A. C. (2017). Disturbance observer based hierarchical control of coaxial-rotor UAV. *ISA Transactions*, 67, 466–475. <https://doi.org/10.1016/j.isatra.2017.01.020>

- Ong, W., Srigrarom, S., & Hesse, H. (2019, 7–11 January). Design methodology for heavy-lift unmanned aerial vehicles with coaxial rotors. In *AIAA Scitech 2019 Forum* (pp. 1–13). San Diego, California. <https://doi.org/10.2514/6.2019-2095>
- Prior, S. D. (2010). Reviewing and investigating the use of coaxial rotor systems in small UAVs. *International Journal of Micro Air Vehicles*, 2(1), 1–16. <https://doi.org/10.1260/1756-8293.2.1.1>
- Prior, S. D., & Bell, J. C. (2011). Empirical measurements of small unmanned aerial vehicle co-axial rotor systems. *Journal of Science and Innovation*, 1(1), 1–18.
- Prouty, R. W. (2002). *Helicopter performance, stability and control*. Krieger Publishing Company.
- P. S., R., & Jeyan, M. L. (2020). Mini Unmanned Aerial Systems (UAV) – a review of the parameters for classification of a Mini UAV. *International Journal of Aviation, Aeronautics, and Aerospace*, 7(3). <https://doi.org/10.15394/ijaaa.2020.1503>
- Ramasamy, M. (2013). Measurements comparing hover performance of single, coaxial, tandem, and tilt-rotor configurations. In *69th Annual Forum Proceedings – AHS International*, 4, 2439–2461. Vertical Flight Society (VFS).
- Ramesh, P. S., & Muruga Lal Jeyan, J. V. (2021). Terrain imperatives for Mini unmanned aircraft systems applications. *International Journal of Intelligent Unmanned Systems*. <https://doi.org/10.1108/IJIUS-09-2020-0044>
- Rand, O., & Khromov, V. (2010). Aerodynamic optimization of coaxial rotor in Hover and axial flight. In *27th Congress of the International Council of the Aeronautical Sciences 2010*, ICAS 2010, 2, 893–905.
- Saito, S., & Azuma, A. (1981). A numerical approach to co-axial rotor aerodynamics. In *Seventh European Rotorcraft and Powered Lift Aircraft Forum*, 42, 1–18.
- Singh, P., & Venkatesan, C. (2013). Experimental performance evaluation of coaxial rotors for a micro aerial vehicle. *Journal of Aircraft*, 50(5), 1465–1480. <https://doi.org/10.2514/1.C031971>
- Thiele, M., Obster, M., & Hornung, M. (2019). Aerodynamic modeling of coaxial counter-rotating UAV propellers. In *8th Biennial Autonomous VTOL Technical Meeting and 6th Annual Electric VTOL Symposium 2019*. Mesa, Arizona, USA. The Vertical Flight Society.
- US Department of Defense. (2013). *Unmanned systems integrated roadmap*. Govt of USA (US Department of Defense).
- Valavanis, K. P., & Vachtsevanos, G. J. (2015). Military and civilian unmanned aircraft. In *Handbook of unmanned aerial vehicles*. Springer. https://doi.org/10.1007/978-90-481-9707-1_47
- Venkatesan, C. (2015). *Fundamentals of helicopter dynamics*. CRC Press. <https://doi.org/10.1115/1.3424469>
- Wang, F., Cui, J., Chen, B. M., & Lee, T. H. (2015). Flight dynamics modeling of coaxial rotorcraft UAVs. In *Handbook of unmanned aerial vehicles*. Springer. <https://doi.org/10.1007/978-90-481-9707-1>
- Yana, J., & Rand, O. (2012). Performance analysis of a coaxial rotor system in Hover: Three points of view. In *28th Congress of the International Council of the Aeronautical Sciences 2012*, ICAS 2012, 2, 1442–1451.
- Yuan, X., & Zhu, J. (2015, January). Comprehensive modeling and analysis of an unmanned coaxial helicopter. In *AIAA Guidance, Navigation, and Control Conference* (pp. 1–16). American Institute of Aeronautics and Astronautics. <https://doi.org/10.2514/6.2015-0593>

Notations

A –	rotor disk area (for one rotor), m^2 ;	N_b –	number of blades (for one rotor);
a –	lift curve slope;	n –	revolutions per minute;
C_d –	drag coefficient;	P –	rotor power, kW ;
C_{d0} –	minimum or zero-lift profile drag coefficient;	Q –	rotor torque, Nm ;
C_l –	lift coefficient;	R –	blade radius, m ;
$\overline{C_l}$ –	mean lift coefficient;	T –	rotor thrust, N ;
C_p –	$P/\rho A \Omega^3 R^3$;	V_{tip} –	rotor tip velocity, m/s ;
C_Q –	$Q/\rho A \Omega^2 R^2$;	v –	induced velocity, m/s ;
C_T –	$T/\rho A \Omega^2 R^2$;	W –	slipstream velocity;
C –	blade chord, m ;	Θ –	blade pitch, rad ;
FM –	rotor system figure of merit;	ρ –	air density, kg/m^3 ;
H/D –	non-dimensional inter-rotor spacing distance;	Σ –	rotor solidity, $Nb c/\pi R$;
K –	rotor-induced power factor (single rotor);	\varnothing –	inflow angle, rad ;
k_{int} –	induced power interference factor for coaxial rotors.	Ω –	rotational speed of the rotor, rad/s

Subscripts and superscripts

L –	lower rotor;
U –	upper rotor;
Eq –	equivalent.